Supplement of Atmos. Meas. Tech., 18, 7853–7863, 2025
https://doi.org/10.5194/amt-18-7853-2025-supplement

Atmospheric Measurement Techniques
Open Access
EGU

Supplement of

CrystalTrace: a Monte Carlo raytracing algorithm for radiative transfer in cirrus clouds with oriented ice crystals

Linda Forster et al.

Correspondence to: Linda Forster (linda.i.forster@jpl.nasa.gov)

S1 Additional CrystalTrace Simulations for Varying Fraction of Oriented Crystals

Mixtures of ice crystal plates with random and preferred orientations, forming a 22° halo together with sundogs, were simulated with CrystalTrace. Figure S1 shows simulations for an increasing fraction of oriented ice crystals from 0% (a) to 100% (f) for the upper hemisphere. The oriented ice crystal plates with an aspect ratio of 0.5 have a vertical c-axis and are oscillating with a standard deviation of 1°. The simulations were performed for a wavelength of 550 nm, a solar zenith angle of 60° and a cirrus optical thickness of 0.8. Here, an aerosol-free atmosphere was assumed. The cirrus cloud in Figure S1a contains only randomly oriented plates which produce a 22° and a 46° halo. A fraction of oriented columns of 20% already shows both sundogs, the parhelic circle with the 120° parhelia and the circumzenithal arc above the sun. As the fraction of oriented crystals increases, the sundogs and other scattering features produced by the oriented crystals intensify. Simultaneously, the brightness of the 22° and a 46° halo is decreasing. In this representation the 46° halo disappears at a fraction of 60% oriented plates while the 22° halo disappears at a fraction of 100% oriented ice crystal plates.

Mixtures of ice crystal columns with random and preferred orientations, forming a 22° halo together with an upper tangent arc, were simulated with CrystalTrace. Figure S2 shows results for an increasing fraction of oriented ice crystals from 0% (a) to 100% (f) for the upper hemisphere. The oriented ice crystal columns with an aspect ratio of 2.5 have a horizontal c-axis and are oscillating with a standard deviation of 1°. The simulations were performed for a wavelength of 550 nm, a solar zenith angle of 60° and a cirrus optical thickness of 0.8 similar to Fig. S1. Figure S2 shows polar plots of the upper hemisphere with the sun at a solar azimuth angle of 270° for an increasing fraction of oriented ice crystals. The cirrus cloud in Fig. S2a contains only randomly oriented columns which produce a 22° halo and a faint 46° halo. A fraction of oriented crystals of 20% already shows the upper and lower tangent arc. As the fraction of oriented columns increases, the brightness of the upper and lower tangent arc increases and the wings of the arcs become more pronounced. Starting from an oriented crystal fraction of 40% the circumhorizontal arc is visible in this representation. Similar to Fig. S1 the 22° halo is still visible for 80% oriented columns and the upper and lower tangent arc are visible already for a fraction of 20% oriented crystals in this representation.

S2 Additional CrystalTrace Simulations for Varying Orientation Parameter

Figure S3 shows how sundogs transition into a 22° halo when the width of the orientation distribution is gradually increased. Starting with an orientation parameter $\sigma_{\beta,\mathrm{Euler}}$ of 5° in panel (a), only the parhelia at 22° and 120° are visible. As soon as the orientation parameter exceeds 10°, parts of the 22° halo become visible along the almucantar plane. For an orientation parameter of 50° and above the 22° halo starts filling in along the principal plane as well and appears very similar to a 22° halo produced by randomly oriented crystals. For reference, Fig. S3f shows results for ice crystal plates with completely random orientation.

Figure S4 illustrates CrystalTrace simlations similar to Fig. S3 but for the lower hemisphere, i.e. from an airborne or satellite perspective. Here, the optical thickness of the cirrus layer is set to 10. The sub-sun together with the parhelia are visible. For an increasing orientation parameter, the angular width of the subsun and parhelia is increasing. At the same time, their brightness is significantly reduced. This is in contrast to the upper hemisphere where the brightness of the halo display remains similar, while the scattering features transition from the parhelia to a 22° halo.

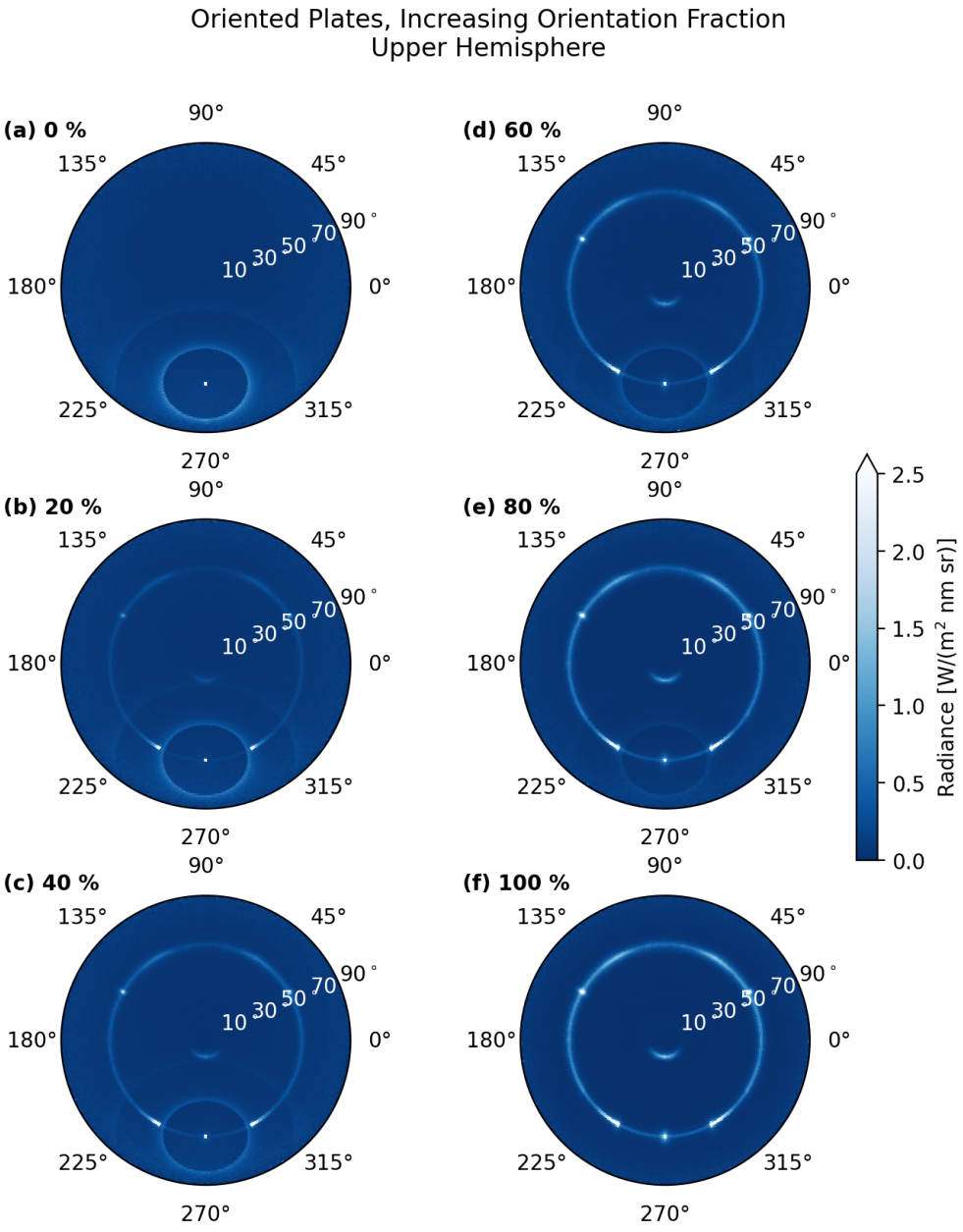

Figure S1: Radiative transfer simulations of a cirrus cloud containing ice crystal plates using libRadtran's MYSTIC solver combined with CrystalTrace for 10^7 photons. An SZA of 60° and an azimuth angle of 270° were chosen. A cirrus optical thickness of 1 and an aspect ratio of 0.5 were chosen for the ice crystal plates. The simulations were performed for different fractions of randomly oriented ice crystals and ice crystals oriented with a vertical c-axis with a orientation parameter of 1°. The fraction of oriented crystals increases from 0% in (a) to 100% in (f).

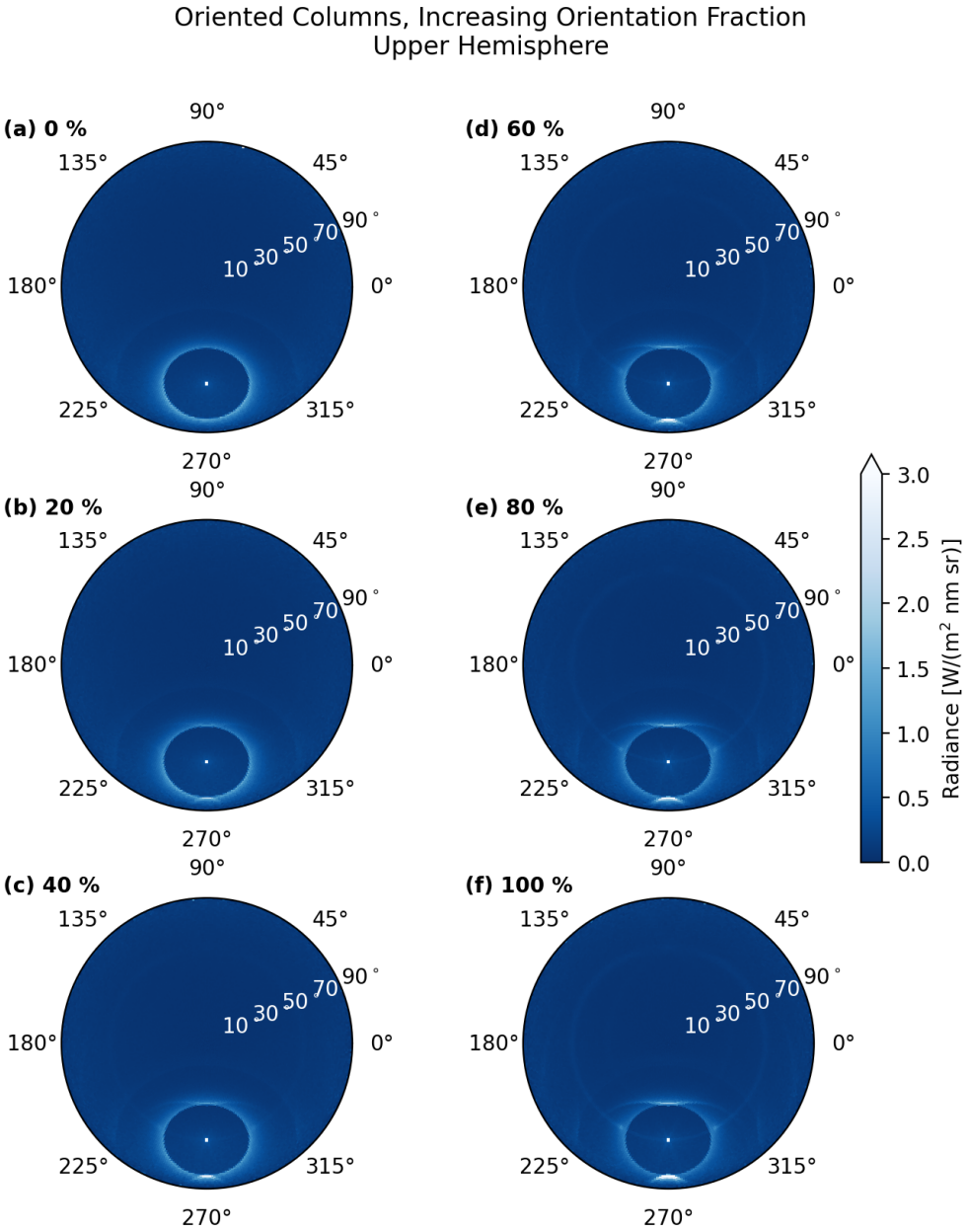

Figure S2: As Fig. S1 but for ice crystal columns with an aspect ratio of 2.5. Randomly oriented columns were mixed with columns oriented with a horizontal c-axis and a orientation parameter of 1°. The fraction of oriented crystals increases from 0% in (a) to 100% in (f).

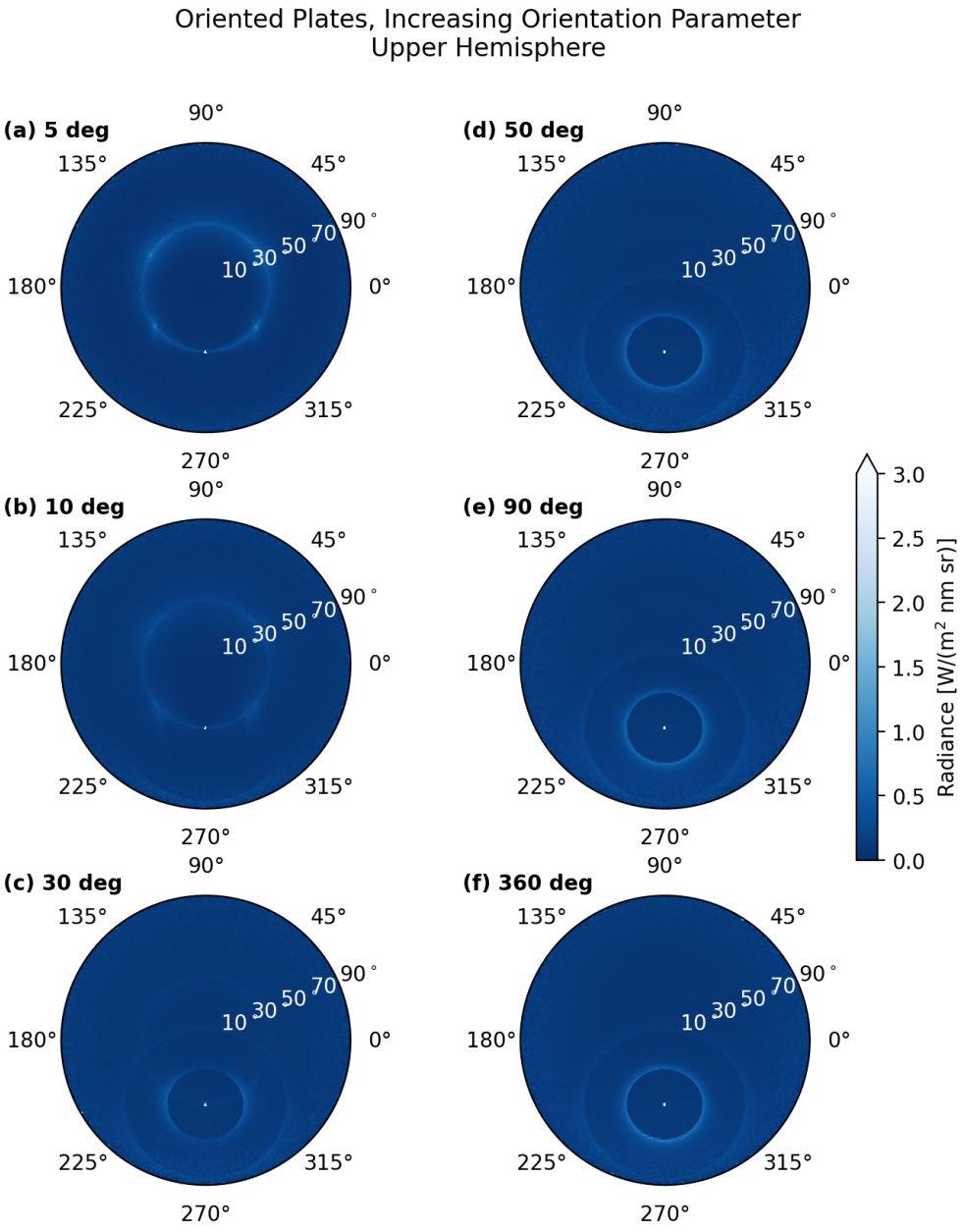

Figure S3: Radiative transfer simulations of a cirrus cloud containing ice crystal plates using libRadtran's MYSTIC solver combined with CrystalTrace for 10^7 photons. An SZA of 40° and an azimuth angle of 270° were chosen. A cirrus optical thickness of 1.0 and an aspect ratio of 0.5 were chosen for the ice crystal plates. The simulations were performed for 100% oriented crystals with a orientation parameter ranging from 5° in (a) to 90° in (e). The results in panel (f) are simulated for plates with completely random orientation.

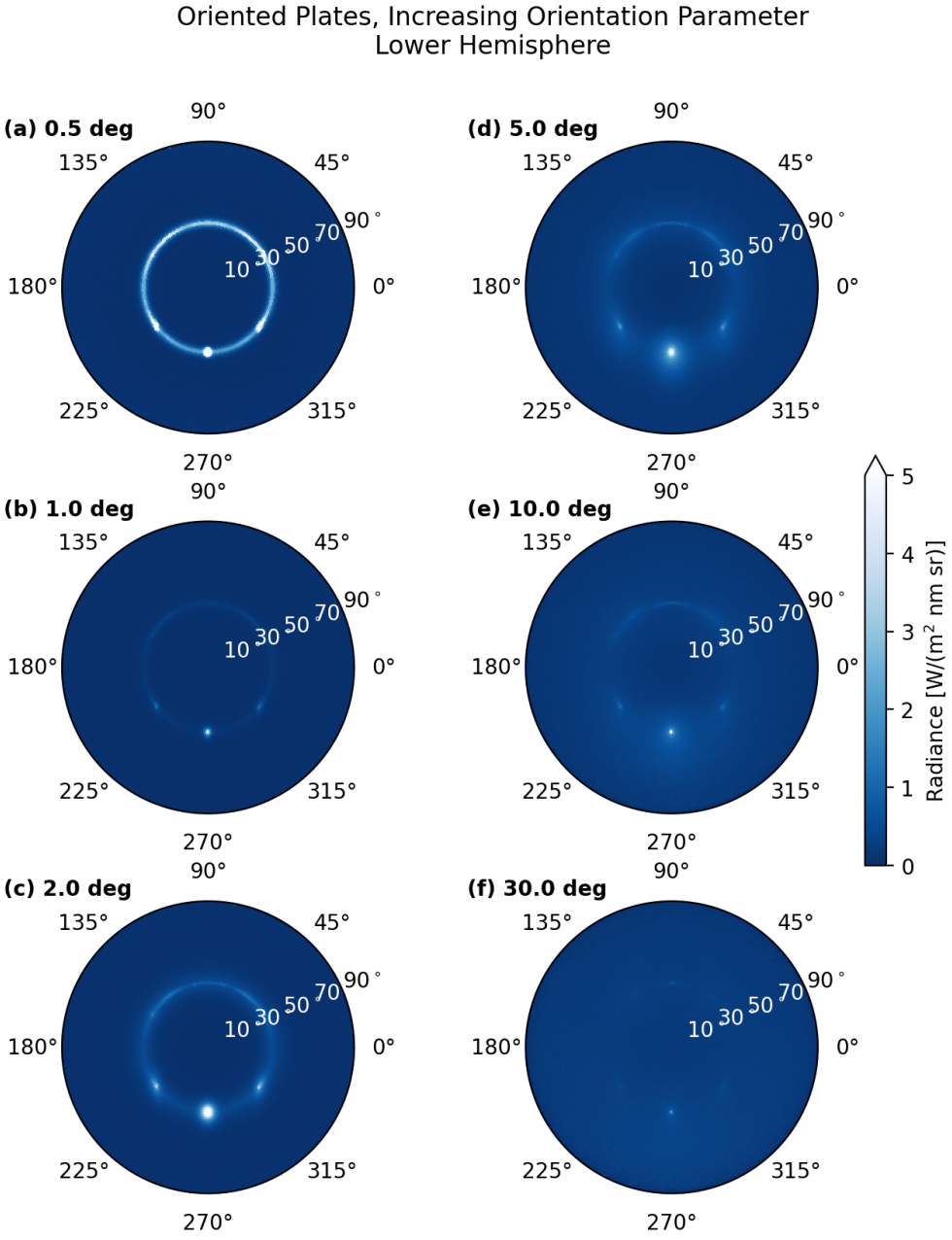

Figure S4: As Fig. S3 but for the lower hemisphere, a cirrus optical thickness of 10 and orientation parameters increasing from 0.5° (a) to 30° (f).

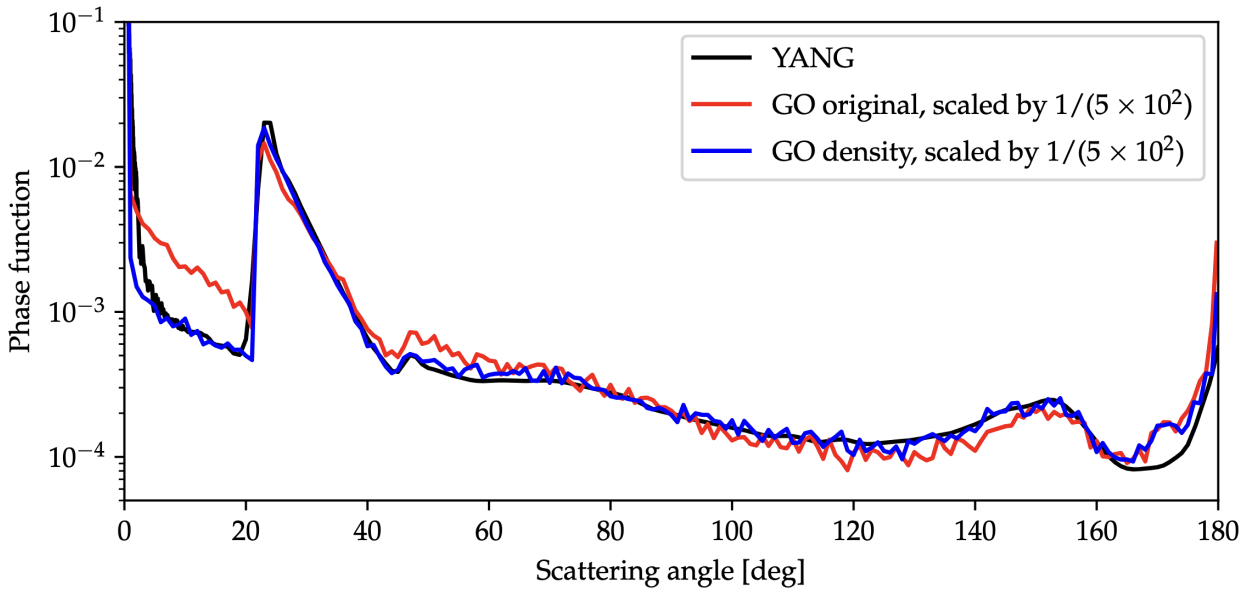

Figure S5: Phase functions calculated with the raytracing code described in Macke et al. (1996) based on the original version (red) and the corrected version using the photon density instead of a fixed photon number (blue), which is referred to as the "GO bug-fixed version" in Fig. 6 of the main manuscript. As a reference, the phase function of the YANG database (black) is shown for the same wavelength of 550 nm and the same ice crystal: a single ice crystal column with aspect ratio AR = 14.4 and maximum dimension D = 1 × 104 μm.

S3 Additional details on the "bug-fixed" version of the GO raytracing code

Figure S5 shows the scattering phase functions calculated with the GO raytracing code in comparison with the phase function of the YANG database at a wavelength of 500 nm for the same columnar ice crystal with AR = 14.4 and a maximum dimension of D = 1 × 104 μm. The red curve represents the phase function calculated using the original raytracing code as described in Macke et al. (1996). In comparison with the phase function of the YANG database (black curve), GO shows significantly larger values for scattering angles inside the 22° halo for an identical ice crystal size and aspect ratio. For compact ice crystals, however, the GO and YANG scattering phase functions are in good agreement (not shown). For growing columns and plates with aspect ratios increasingly deviating from 1, the difference between the GO and YANG phase functions is increasing for smaller scattering angles. The reason for this behavior of the GO raytracing code was identified by Konoshonkin et al. (2016): "incident rays are emitted from a rectangular bounded the particle projection. With a change of particle orientation, the area of the rectangular is variable. This area variation must be taken into account." In correspondence with A. Macke the bug was fixed by providing the photon density as a constant instead of the number of photons to trace. For every orientation of the crystal the number of photons is calculated from the photon density multiplied by the area of the bounding rectangle of the projected ice crystal. The blue line in Fig. S5 shows the result of the corrected GO code using a constant photon density as input parameter. Compared with the YANG phase function of the same ice crystal size and shape, which is depicted in black, and the phase functions agree well.

S4 Bibliography

Konoshonkin, A. V., N. V. Kustova, A. G. Borovoi, Y. Grynko, and J. Förstner, 2016: Light scattering by ice crystals of cirrus clouds: comparison of the physical optics methods. J. Quant. Spectrosc. Radiat. Transfer, 182, 12–23, doi:10.1016/j.jqsrt.2016.05.006.

Macke, A., J. Mueller, and E. Raschke, 1996: Single scattering properties of atmospheric ice crystals. J. Atmos. Sci., 53 (19), 2813–2825, doi:10.1175/1520-0469(1996)053⟨2813:SSPOAI⟩ 2.0.CO;2.